Ab Initio Dynamic Study of the Reaction of Cl_2LaR (R = H, CH_3) with H_2

Christophe Raynaud, Jean-Pierre Daudey, Franck Jolibois, and Laurent Maron*

Laboratoire de Physique Quantique (UMR 5626), IRSAMC, Université Paul Sabatier, 118 Route de Narbonne, 31062 Toulouse Cedex 4, France

Received: February 14, 2005; In Final Form: November 8, 2005

In this paper, a comparison between "static" and "dynamic" determination of the thermodynamic ($\Delta_r F°$) and kinetic data ($\Delta_r F^{\#}$) for the reaction of Cl_2LaR (R = H, CH_3) and H_2 is given. A difference is obtained in the case of the reaction between Cl_2LaH and H_2 and can be attributed to a failure of the "static" approach based on the harmonic approximation. The influence of the zero point energy correction is also analyzed but does not explain the 30% difference between the two calculated activation energies. The influence of the flatness of the potential energy surface around the transition state is proved as no such an effect is observed for the reaction of Cl_2LaCH_3 and H_2.

Introduction

Lanthanide chemistry has been of increasing interest from the beginning of the 1980s due to the work of Watson et al. who showed that Cp^*_2LuH ($Cp^* = C_5Me_5$) or $Cp^*_2LuCH_3$ react rapidly with H_2 or methane.[1] The authors obtained kinetic data for the reactions with the relative rates dependent on different metals (Sc, Y, and Lu).

$$Cp^*_2LuH + H_2 \leftrightarrow Cp^*_2LuH + H_2 \quad (1)$$

$$Cp^*_2LuCH_3 + H_2 \leftrightarrow Cp^*_2LuH + CH_4 \quad (2)$$

The first reaction (eq 1) is formally a hydride exchange, whereas the second one (eq 2) is the reaction of formation of the hydride. These reactions have been postulated to proceed through σ-bond metathesis transition state.

Recently, these reactions have been investigated by different groups theoretically.[2,3] It has been shown that the reaction is a σ-bond metathesis proceeding through a four-center transition state. In agreement with the experiment, the activation barrier is found to be small for both reactions. The calculated thermodynamic ($\Delta_r F°$) and kinetic ($\Delta_r F^{\#}$) data, where $\Delta_r F^{\#}$ is the free energy difference between the transition state (TS) and the reactants and is the activation barrier for the reactions, can be estimated by including the electronic energy or by estimating the temperature effect in order to obtain the free energy. In the latter case, this effect is usually estimated by applying the harmonic approximation[4] on the specific points of the potential energy surface (PES). It is well-established that this approximation can fail when flat potential energy surfaces are considered. In this paper, this method will be called the "static" calculation. A more rigorous way of determining the temperature effect is based on a dynamical approach for which temperature is explicitly controlled by simulating the canonical ensemble by means of thermostat[5] in the molecular dynamics simulation scheme. The thermodynamic and kinetic data can then be determined by employing a constraint[6] which should correspond to the reaction coordinate. However, if the propagation of the nuclei is classical, quantum nuclear effects such as the zero point energy (ZPE) correction are not a priori taken into account. Anharmonic ZPE can be estimated in such dynamical calculations by using an adiabatic switching between a harmonic Hamiltonian and the real Hamiltonian during a simulation.[7] However, to the best of our knowledge, this approach has not yet been applied to transition states, and this will be the aim of a forthcoming paper.[8] For the comparison between "static" and "dynamic" calculations, the influence of zero point corrections to the energy will be discussed. Moreover, as the aim of this paper is to compare the two approaches and not to compare with experiment, the calculations have been carried out on Cl_2LaH and Cl_2LaCH_3 without taking into account the possibility of tunneling effect. In this paper, the dynamic approach is based on ab initio molecular dynamics[9] using Gaussian type basis functions[10] in order to describe the electronic wave function. Thermodynamic and kinetic data have been obtained using constrained molecular dynamics simulations within the "blue moon" approach.[11]

Methodological Aspects

From free (unconstrained) ab initio molecular dynamics simulations, two important thermodynamic quantities for a chemical process, the entropy and the free energy, cannot, in general, be derived from a statistical average. These are global properties that depend on the extent of the phase (or configuration) space accessible to the molecular system during the simulation. The probability of finding the system in a transition-state region is so small that no relative free energies of a chemical process can be calculated by natural molecular dynamics simulations. Several statistical mechanical procedures circumvent this problem. For instance, the "umbrella sampling" method,[12,13] which adds a coordinate-dependent potential, leads the system to sample a specific region of the phase space. Another approach, the blue moon method,[11] also allows relative free energies for the chemical process to be estimated, by sampling the phase space along a defined reaction pathway. By means of thermodynamic integration,[14] the free energy difference is obtained as

$$F(\xi_2) - F(\xi_1) = \int_{\xi_1}^{\xi_2} d\xi' \left\langle \frac{\partial H}{\partial \xi} \right\rangle_{\xi'}$$

* To whom correspondence should be addressed. E-mail: laurent.maron@irsamc.ups-tlse.fr.

10.1021/jp050771v CCC: $33.50
Published on Web 12/07/2005

where H is the Hamiltonian of the system, $\xi(\mathbf{r})$ is the reaction coordinate and $\langle ... \rangle_\xi$ is an ensemble average evaluated at $\xi(\mathbf{r}) = \xi'$. The precedent conditional average could be estimated by a time average over a constrained trajectory with the reaction coordinate fixed at a specified value. Recently, generally applicable expressions for the average force of the constraint $f_{\xi'}$, which is the opposite of the integrand (i.e. $-\langle \partial H/\partial \xi \rangle_{\xi'}$), have been outlined,[6,15] and have shown that the bias introduced by the constraint can be corrected by considering the following expression:

$$f_\xi = \frac{\langle Z^{-1/2}(-\lambda + k_B T G)\rangle_\xi}{\langle Z^{-/2}\rangle_\xi}$$

where k_B is the Boltzmann constant, T is the temperature, Z and G are respectively weight and correction factors, and λ is the Lagrange multiplier of the associated holonomic constraint.

Computational Details

In previous studies,[16,17] it has been shown that large core (4f electrons are not treated explicitly) relativistic effective core potentials (RECPs) optimized by the Stuttgart−Dresden[18−20] group are well-adapted to the calculation of the geometries of lanthanide complexes as 4f electrons do not participate in Ln−X bonding. Consequently they were also used in the present study, with their adapted basis sets (extended valence basis set plus a set of polarization functions). Chlorine and carbon atoms were also treated with RECPs in combination with their adapted basis sets (double-ζ quality), augmented by a polarization function.[21] Hydrogen atoms have been described with a 6-31G(d,p) double-ζ basis set.[22] Calculations were carried out at the density functional theory (DFT) level using the hybrid functional B3PW91.[23,24] For static calculations, geometry optimizations were carried out without any symmetry restrictions, the nature of the *extrema* (*minimum* or transition structure) was verified with analytical frequency calculations. All these computations have been performed with the Gaussian 98[25] suite of programs. Free energy differences at room temperature have been estimated using the standard harmonic approximation for static calculations and by means of the blue moon approach for the molecular dynamics ones. Ab initio molecular dynamics simulations with Gaussian type orbitals have been performed with our own code.[10] Fictitious electronic mass was set to 170 au, and equations of motion have been integrated with a time step of 0.25 fs by means of a velocity Verlet[26] scheme. These simulations were performed in the canonical ensemble with Nosé−Hoover chains of thermostats,[5] and holonomic constraints associated to the reaction coordinate have been applied considering the method of undetermined parameters.[27] For each trajectory, thermalization procedure has been performed for at least 6 ps. Then, production simulations have been accomplished for 5−6 ps more. The property of interest (the force of the constraint) has been averaged as a function of time during the production step, and its convergence has been checked at the end of the whole process.

Description of Geometrical Constraints. When dealing with chemical processes, the choice of the constraint can be a difficult task, since the constraint, which must be connected to the reaction coordinate, can be described by several geometrical parameters. For our studies, it is very difficult to find a function that will constrain the TS geometry which can be mainly described by concerted breaking/forming of four bonds. A way to circumvent this problem is to find a simple representation of the reaction coordinate using only a single geometrical parameter. However, an incorrect choice of this type of simple constraint can induce a bias for free energy calculation. Thus, it is important to check the validity of one constraint by comparing the final results with the ones obtained using different constraints. For the first reaction ($Cl_2LaH + H_2$), three kinds of geometrical constraints have been used. The first one corresponds to the projection of the H_aH_b vector on the H_aH_c one (see Chart 1 for atom definitions). The second constraint is associated to the distance between the lanthanum atom and the center of mass of H_2 (H_aH_b). Finally, a third constraint has been defined as the distance between H_b (the "flying" hydrogen) and H_c (the hydride).

CHART 1: Atom Numbering for the Definition of the Geometric Constraints

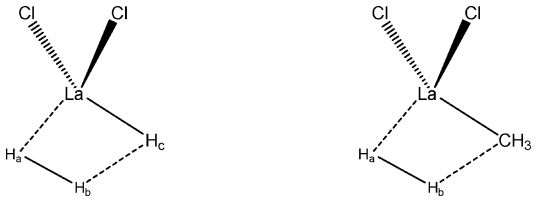

For the second reaction ($Cl_2LaCH_3 + H_2$), the constrained scheme must ensure the description of an asymmetric energy profile and thus one constraint can be applied for each half-part. For the first half of the reaction profile (from reactants to TS), the distance between lanthanum atom and the center of mass of H_2 (H_aH_b) has been used as a geometrical constraint. For the second half (from TS to products), the distance between the lanthanum atom and methyl carbon has been employed. Another way to describe the whole profile by means of only one constraint is to employ a projection scheme (H_aH_b vector projected on the H_aC vector) similar to the one used for the first reaction.

Results and Discussion

Reaction of Cl_2LaH with H_2. For the sake of clarity and simplicity, only the dynamic energy profile obtained using the projection constraint will be discussed. Calculations using the other constraints give the same thermodynamic and kinetic result: the differences between the activation barriers obtained with these constraints were less than 0.1 kcal·mol^{-1}. The schematic free energy profiles obtained with the "static" and dynamical approaches are presented in Figure 1. As can be seen, the energy barrier obtained with the static approach is overestimated with respect to the dynamic one. Indeed, within the harmonic approximation, the calculated energy barrier is found to be 11.2 kcal·mol^{-1} whereas the barrier within the dynamic approach is calculated to be 6.2 kcal.mol^{-1}. To make a relevant comparison between the two calculations, it is essential to compare the two pathways in order to ensure that the same transition state is obtained with both methods. It is also necessary to compare the geometries obtained in both calculations for the reactants. In the dynamic case, the geometry is based on the

CHART 2: Four-Center Transition-State Geometrical Parameters[a]

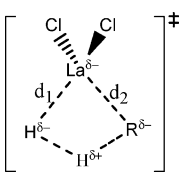

[a] R can be either H or CH_3.

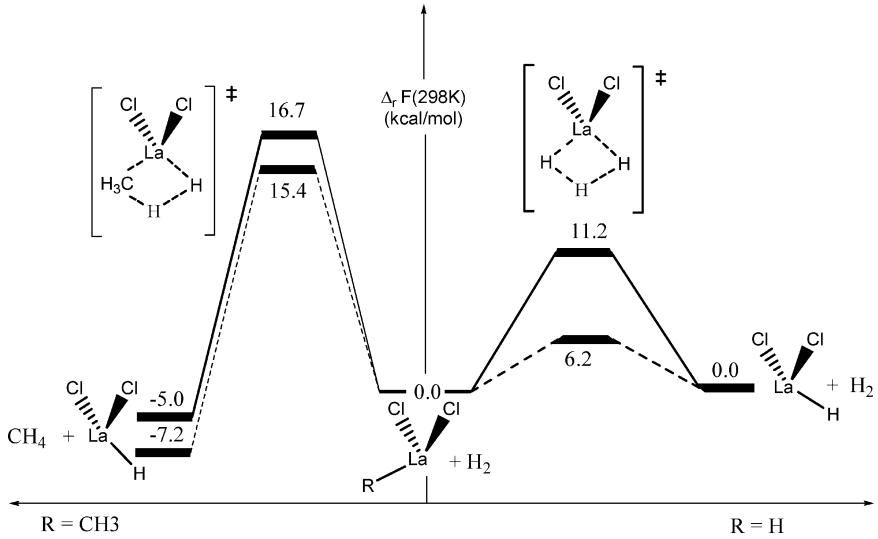

Figure 1. Schematic free energy profile of the two reactions using both static and dynamic approaches. The ZPE is included in the static results. The dashed line corresponds to the dynamic results. The energy is given in kcal·mol^{-1}.

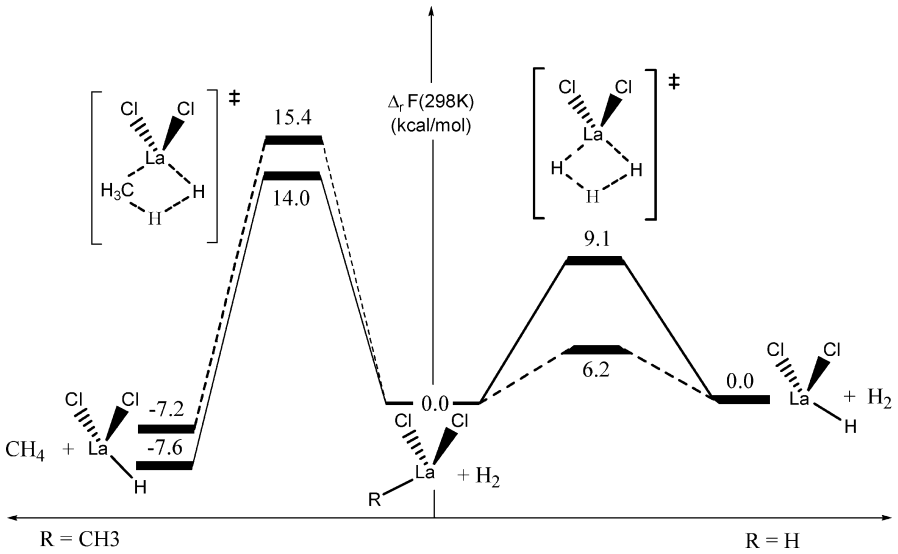

Figure 2. Schematic free energy profile of the two reactions using both static and dynamic approaches. The ZPE is not taken into account for the static results. The dashed line corresponds to the dynamic results. The energy is given in kcal·mol^{-1}.

averaged bond distances and bond angles. For Cl_2LaH, the static geometry is described by a La−H bond length of 2.11 Å and a Cl−La−Cl angle of 116°. The corresponding geometry in the dynamic calculation is very close to the previously described one with a La−H bond length of 2.12 ± 0.05 Å and a Cl−La−Cl angle of 118 ± 6°.

As expected, the calculated geometries of the reactants are very similar with both methods. The geometry of the four-center transition state can be described by the parameter presented in Chart 2.

From dynamic calculations, the d_1 and d_2 distances are equal to 2.26 ± 0.08 Å. This value is identical to the one obtained by static approach (2.26 Å). The small geometrical differences found for the reactant cannot explain the large discrepancy between the two calculated activation barriers and since the two pathways are almost identical. Therefore, it is concluded that the static and dynamic energy profile difference is due to the way the activation barrier is calculated. As mentioned in the Introduction, standard classical propagation of the nuclei in ab initio molecular dynamics simulation does not take into account nuclear quantum effects such as ZPE corrections. The latter is included in our "static" calculation, which leads to the question: does this difference come only from the inclusion of ZPE correction?

Several possible ways to answer this question can be listed. First, the zero point energy correction can be estimated in dynamic simulations within an adiabatic switching approach.[7] However, as already mentioned, such a method has not yet been applied to transition states. Work is in progress to consider this switching and will be presented in a separate paper. As a pure quantum propagation is not feasible (mainly due to the size of the system), the easiest way to determine whether the ZPE correction is responsible of the discrepancy or not is not to consider such correction in the static calculation.

Removing this correction from the static calculation leads to an activation barrier of 9.1 kcal·mol^{-1} to be compared with a value of 6.2 kcal·mol^{-1} from dynamic calculation (see Figure 2). Thus, the activation barrier is reduced by ∼30% when one goes from static to dynamic calculations. Thus the influence of the ZPE correction is an important factor, but it does not explain the whole difference. Second, the discrepancy is due to a failure of the harmonic approximation used to determine the thermal correction in static calculation. As it is well-known that such failure is very often based on a flat energy surface,[28,29] the PES

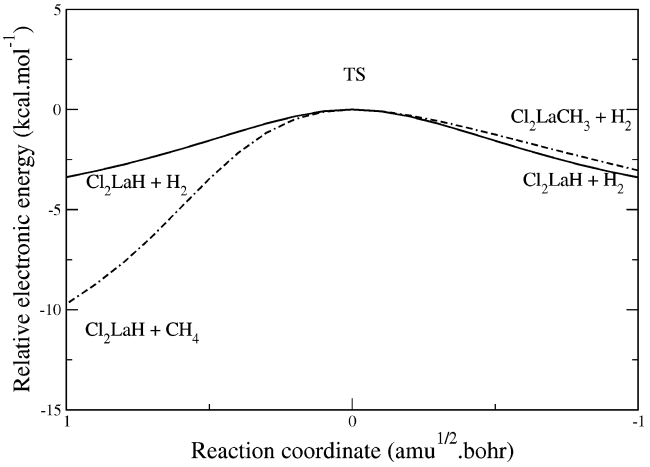

Figure 3. Shape of the electronic PES for both reactions. The H−H exchange is represented in solid line and the H−CH_3 exchange in dashed line. The energy is given in kcal·mol^{-1} and the reaction coordinate in amu$^{1/2}$.bohr.

around the transition state has been plotted using the intrinsic reaction coordinate (IRC) method.[30]

As can be seen from Figure 3, the PES corresponding to the H/H exchange is very flat along the intrinsic reaction coordinate. Moreover, an analysis of the vibrational spectrum calculated at the transition state using both approaches (static and dynamic) shows that a significant number (6) of low frequencies (below 500 cm^{-1}) are present (see Figure 4). The dynamic vibrational spectrum is obtained by calculating the Fourier transform of the velocity autocorrelation function.

In transition-state theory, this certainly would be consistent with a flat surface, not only along the reaction coordinate but also along other orthogonal degrees of freedom. This flatness around the transition state makes then the harmonic approximation, which is used to estimate thermal correction as well as the entropy, questionable. Moreover the good agreement between static and dynamic vibrational spectra validates the choice and correctness of the constraint used (the projection one).

As can be seen from Figure 5, the dynamical free energy profile, along the reaction coordinate, is also very flat. Moreover, the flatness of the PES perpendicular to the reaction coordinate has already been discussed based on the vibrational spectrum (Figure 4). Thus, it is not surprising that the harmonic approximation failed in representing such a flat free energy surface. To assess the harmonic approximation failure, a similar study has been carried out on $Cl_2LaCH_3 + H_2$.

Reaction of Cl_2LaCH_3 with H_2. The results obtained for the previously described reaction can lead to two different questions. The first one is based on the influence of the flatness of the PES around the TS, and the second one, which is related to the first one is, can the discrepancy be the same for a different kind of a reaction? To try to answer these questions, the reaction $Cl_2LaCH_3 + H_2$ has been investigated using both approaches. It is shown that the activation barrier of this reaction is higher than the previous one if one considers static calculations. For dynamic computations, the constraint has been considered to be the same as for the previous reaction (projection vector). The energy profiles are presented in Figure 1. Both methods agree that the activation barrier is higher for this reaction than for the previous one. In contrast to the first considered reaction, the calculated activation barriers are in good agreement in both methods. Indeed, the static activation barrier is calculated to be 16.7 kcal·mol^{-1} and the dynamic one is found to be 15.4 kcal·mol^{-1}. It seems that the harmonic approximation is efficient in this particular case. As for the reaction of Cl_2LaH with H_2, the geometry of the reactants, products, and transition state are calculated even though the activation barrier are almost identical.

The static geometry of the reactant can be described by a La−C bond length of 2.47 Å and a Cl−La−Cl angle of 118°. The corresponding geometry in the dynamic calculation is very close to the previously one with a La−C bond length of 2.48 ± 0.05 Å and a Cl−La−Cl angle of 119 ± 10°. In the same manner, the d_1 and d_2 distances in the TS compare well between the two calculations (d_1, 2.29 Å vs 2.27 ± 0.07 Å; d_2, 2.55 Å vs 2.61 ± 0.07 Å). The pathways determined by both methods are very similar. For this reaction, the two calculated activation barriers are close but the ZPE correction must be removed from the static free energy in order to get a pertinent comparison. When this term is removed from static free energy, the activation barrier is now 14.0 kcal·mol^{-1} (see Figure 2). As for the reaction of Cl_2LaH with H_2, the ZPE correction does not introduce a major difference between static and dynamic calculations. If the IRC profile is considered (Figure 3), one-half of the energy profile (IRC = 0 to −1) is similar to the one obtained for the first reaction. This part of the profile corresponds to the attack of the H_2 molecule on the lanthanum complexe (Cl_2LaR, R = H or CH_3). However, for the second half of the IRC profile (IRC = 0 to 1), the slope of the curve is more pronounced in the case of methane formation. On the other hand, the shape of the free energy profile obtained from dynamic simulations (Figure 4) exhibits a major difference with respect to the analogous curve associated to the first reaction. Indeed, along the reaction coordinate, the free energy surface is less flat than for the $Cl_2LaH + H_2$ reaction. Moreover, concerning the

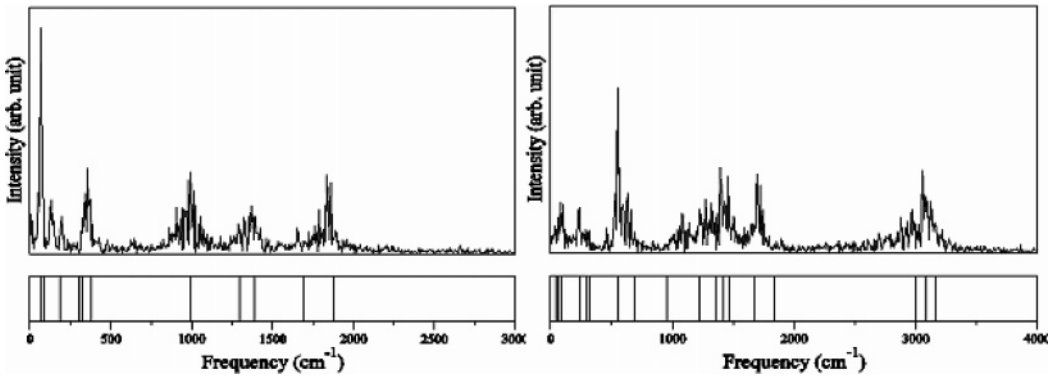

Figure 4. Spectra of the motions of the constrained molecular dynamics at the transition state for the $Cl_2LaH + H_2$ (on the left) and the $Cl_2LaCH_4 + H_2$ (on the right) reactions, obtained with the velocity autocorrelation function. The lower graphs show all of the corresponding frequencies obtained by static calculations.

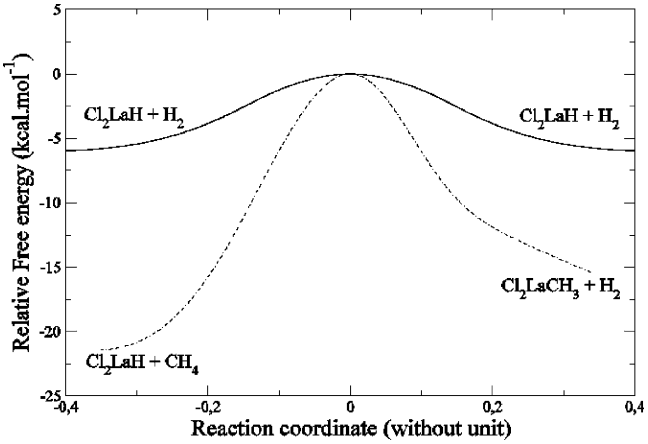

Figure 5. Shape of the free energy surface obtained from dynamic simulations for both reactions. The H−H exchange is represented in solid line and the H−CH_3 exchange in dashed line. The energy is given in kcal·mol^{-1}. The dimensionless reaction coordinate corresponds to the projection of the H_aH_b vector on the H_aR vector (see Computational Details) and has no unit. The reaction coordinate associated to the TS structure has been translated to the origin.

orthogonal normal modes (vibration spectrum shown in Figure 4, right), the percentage of low frequencies present in the vibrational spectrum of the associated TS is less important than in the previous case. A precise analysis of these low-frequency normal modes shows that the carbon atom is involved introducing a mass effect which partially restricts nuclear motions. Thus, it will be more difficult for the molecular system to reach the anharmonic region of the PES and the latter effects will be less pronounced for the estimation of free energy. If all these observations are taken into account, one can conclude that the flatness of the PES is less manifest and the harmonic approximation seems correct in this case. This is coherent with the calculation of static and dynamic energy barriers that we found are almost equal.

Conclusion

In this paper, a comparison between the "static" and "dynamic" approaches to determine the thermodynamic ($\Delta_r F°$) and kinetic (energy barrier, $\Delta_r F^{\#}$) values has been performed in the case of reactions involving a lanthanide center. It is possible to show that in the case of the reaction of Cl_2LaH with H_2, the static determination of the activation barrier is overestimated by 30% and is due to a failure of the harmonic approximation. This has been attributed to the well-known problem of the flatness of the potential energy surface around the transition state. The effect of the ZPE correction results in an overestimation of the barrier by about 10%, but the ZPE correction cannot explain the entire discrepancy. It however indicates that such an effect should be included in ab initio molecular dynamic studies. Work is in progress to include this effect by means of adiabatic switching. The results described in this paper also show that this overestimation is not systematic by considering a reaction of H_2 with Cl_2LaCH_3. In this case, the static results are in quantitative agreement with the dynamic one. The main difference with the previous reaction is that the PES around the TS is less flat. This characteristic property allows us to conclude that the harmonic approximation is correct in this case. The effect of the ZPE correction is not important for this reaction.

The results obtained within our dynamic approach are very encouraging, and further development will be devoted to the treatment of more realistic systems. In particular, implementation of the QM/MM method[31,32] and the effective group potential[33] (EGP) for the real reaction is being studied.

Acknowledgment. The authors would like to thank Dr. Florent Calvo for fruitful discussion on the problem of the ZPE determination using classical propagation scheme. The authors would also like to thank Prof. Richard A. Andersen and Alejandro Ramirez-Solis for fruitful help to write this manuscript. The authors gratefully acknowledge the national French computing centers CINES and CALMIP for a generous donation of computing times. This work is supported by the grant from the French Ministry of Research (ACI No. 4009).

Supporting Information Available: Cartesian coordinates of all the complexes described in the article. This material is available free of charge via the Internet at http://pubs.acs.org.

References and Notes

(1) Watson, P. L.; Parshall, G. W. *Acc. Chem. Res.* **1985**, *18*, 51.
(2) Ziegler, T.; Folga, E. *J. Am. Chem. Soc.* **1993**, *115*, 636.
(3) Maron, L.; Perrin, L.; Eisenstein, O. *J. Chem. Soc., Dalton Trans.* **2002**, *534*.
(4) McQuarrie, D. A. *Statistical Thermodynamics*; Harper and Row: New York, 1973.
(5) Hoover, W. G. *Phys. Rev. A* **1985**, *31*, 1695.
(6) Sprik, M.; Ciccotti, G. *J. Chem. Phys.* **1998**, *109*, 7737.
(7) Huang, J.; Valentini, J. J.; Muckerman, J. T. *J. Chem. Phys.* **1995**, *102*, 5695.
(8) Raynaud, C.; Daudey, J.-P.; Maron, L.; Jolibois, F. To be submitted for publication.
(9) Car, R.; Parrinello, M. *Phys. Rev. Lett.* **1985**, *55*, 2471.
(10) Raynaud, C.; Maron, L.; Daudey, J.-P.; Jolibois, F. *Phys. Chem. Chem. Phys.* **2004**, *6*, 4226.
(11) Carter, E. A.; Ciccotti, G.; Hynes, J. T.; Kapral, R. *Chem. Phys. Lett.* **1989**, *156*, 472.
(12) Torrie, G. M.; Valleau, J.-P. *Chem. Phys. Lett.* **1974**, *28*, 578.
(13) Torrie, G. M.; Valleau, J.-P. *J. Comput. Phys.* **1977**, *23*, 187.
(14) Frenkel, D.; Smit, B. *Understanding Molecular Simulation*; Academic Press: New York, 1996.
(15) Den Otter, W. K.; Briels, W. J. *J. Chem. Phys.* **1998**, *109*, 4139.
(16) Maron, L.; Eisenstein, O. *J. Phys. Chem. A* **2000**, *104*, 7140.
(17) Maron, L.; Eisenstein, O. *New J. Chem.* **2001**, *25*, 55.
(18) Dolg, M.; Stoll, M.; Savin, A.; Preuss, H. *Theor. Chim. Acta* **1989**, *75*, 173.
(19) Dolg, M.; Fulde, O.; Kuchle, W.; Neumann, C. S.; Stoll, M. *Chem. Phys.* **1991**, *94*, 3011.
(20) Dolg, M.; Stoll, M.; Preuss, H. *Theor. Chim. Acta* **1993**, *85*, 411.
(21) Maron, L.; Teichtel, C. *Chem. Phys.* **1998**, *237*, 105.
(22) Hariharan, P. C.; Pople, J. A. *Theor. Chim. Acta* **1973**, *28*, 213.
(23) Becke, A. D. *J. Chem. Phys.* **1993**, *98*, 5648.
(24) Burke, K.; Perdew, J. P.; Yang, W. In *Electronic Density Functional Theory: Recent Progress and New Directions*; Dobson, J. F., Vignale, G., Das, M. P., Eds.; 1998.
(25) Frisch, M. J.; Trucks, G. W.; Schlegel, H. B.; Scuseria, G. E.; Robb, M. A.; Cheeseman, J. R.; Zakrzewski, V. G.; Montgomery, J. A.; Stratmann, R. E.; Burant, J. C.; Dapprich, S.; Millam, J. M.; Daniels, A. D.; Kudin, K. N.; Strain, M. C.; Farkas, O.; Tomasi, J.; Barone, V.; Cossi, M.; Cammi, R.; Mennucci, B.; Pomelli, C.; Adamo, C.; Clifford, S.; Ochterski, J.; Petersson, G. A.; Ayala, P. Y.; Cui, Q.; Morokuma, K.; Malick, D. K.; Rabuck, A. D.; Raghavachari, K.; Foresman, J. B.; Cioslowski, J.; Ortiz, J. W.; Baboul, A. G.; Stefanov, B. B.; Liu, G.; Liashenko, A.; Piskorz, P.; Komaromi, I.; Gomperts, R.; Martin, R. L.; Fox, D. J.; Keith, T.; Al-Laham, M. A.; Peng, C. Y.; Nanayakkara, A.; Gonzalez, C.; Challacombe, M.; Gill, P. M. W.; Johnson, B. G.; Chen, W.; Wong, M. W.; Andres, J. L.; Head-Gordon, M.; Replogle, E. S.; Pople, J. A. *Gaussian 98*, A.9 ed.; Gaussian: Pittsburgh, PA, 1998.
(26) Verlet, L. *Phys. Rev.* **1967**, *159*, 98.
(27) Kutteh, R.; Straatsma, T. P. *Reviews in Computaionnal Chemistry*; Wiley-VCH: New York, 1998; Vol. 12, p 75.
(28) Rauhut, G. *Phys. Chem. Chem. Phys.* **2003**, *5*, 791.
(29) Schweiger, S.; Rauhut, G. *J. Phys. Chem. A* **2003**, *107*, 9668.
(30) Fukui, K. *J. Phys. Chem.* **1970**, *74*, 4161.
(31) Svensson, M.; Humbel, S.; Froese, R. D. J.; Matsubara, T.; Sieber, S.; Morokuma, K. *J. Chem. Phys.* **1996**, *100*, 19357.
(32) Dapprich, S.; Komaroma, K. S.; Byun, K. S.; Morokuma, K. *J. Mol. Struct. (THEOCHEM)* **1999**, *461*, 1.
(33) Bessac, F.; Alary, F.; Poteau, R.; Heully, J.-L.; Daudey, J.-P. *J. Phys. Chem. A* **2003**, *107*, 9393.